Published in final edited form as:
Nature. ; 474(7353): 640–644. doi:10.1038/nature10188.

De novo cardiomyocytes from within the activated adult heart after injury

Nicola Smart[1,*], **Sveva Bollini**[1,*], **Karina N. Dubé**[1], **Joaquim M. Vieira**[1], **Bin Zhou**[2,3,4], **Sean Davidson**[5], **Derek Yellon**[5], **Johannes Riegler**[6,7], **Anthony N. Price**[8], **Mark F. Lythgoe**[6], **William T. Pu**[2,3], and **Paul R. Riley**[1]

[1]Molecular Medicine Unit, UCL Institute of Child Health, London WC1N 1EH, UK.

[2]Harvard Stem Cell Institute and Department of Cardiology, Children's Hospital Boston, 300 Longwood Avenue, Boston, Massachusetts 02115, USA.

[3]Department of Genetics, Harvard Medical School, 77 Avenue Louis Pasteur, Boston, Massachusetts 02115, USA.

[4]Institute for Nutritional Sciences, Shanghai Institute for Biological Sciences, Chinese Academy of Sciences, China, 20031.

[5]The Hatter Cardiovascular Institute, University College London, London WC1E 6HX, USA.

[6]Centre for Advanced Biomedical Imaging (CABI), Department of Medicine and Institute of Child Health, University College London, London WC1E 6DD, UK.

[7]Centre for Mathematics and Physics in the Life Sciences and Experimental Biology (CoMPLEX), University College London, London WC1E 6BT, UK.

[8]MRC Clinical Sciences Centre, Faculty of Medicine, Imperial College London, London W12 0NN, UK.

Abstract

A significant bottleneck in cardiovascular regenerative medicine is the identification of a viable source of stem/progenitor cells that could contribute new muscle after ischaemic heart disease and acute myocardial infarction[1]. A therapeutic ideal—relative to cell transplantation—would be to stimulate a resident source, thus avoiding the caveats of limited graft survival, restricted homing to the site of injury and host immune rejection. Here we demonstrate in mice that the adult heart contains a resident stem or progenitor cell population, which has the potential to contribute bona fide terminally differentiated cardiomyocytes after myocardial infarction. We reveal a novel genetic label of the activated adult progenitors via re-expression of a key embryonic epicardial gene, Wilm's tumour 1 (*Wt1*), through priming by thymosin β4, a peptide previously shown to

Correspondence and requests for materials should be addressed to P.R.R. (p.riley@ich.ucl.ac.uk)..
*These authors contributed equally to this work.

Supplementary Information is linked to the online version of the paper at www.nature.com/nature.

Author Contributions N.S. carried out the *in vivo* histological assessments of cardiomyocytes and FISH experiments. S.B. carried out the explant and FACS studies and jointly with K.N.D. established the myocardial infarction model and the cell transplantation. J.M.V. carried out the qRT–PCR analyses and assisted with cell transplantation. B.Z. generated the $Wt1^{GFPCre}$ and $Wt1^{CreERT2}$ mice. S.D. and D.Y. performed the two-photon microscopy and Ca^{2+} transient recordings. J.R., A.N.P. and M.F.L. carried out the MRI functional analyses. W.T.P. provided the $Wt1^{GFPCre}$ and $Wt1^{CreERT2}$ mice. P.R.R. established the hypotheses and experimental design, co-analysed data and wrote the manuscript.

Author Information Reprints and permissions information is available at www.nature.com/reprints. The authors declare no competing financial interests. Readers are welcome to comment on the online version of this article at www.nature.com/nature.

restore vascular potential to adult epicardium-derived progenitor cells[2] with injury. Cumulative evidence indicates an epicardial origin of the progenitor population, and embryonic reprogramming results in the mobilization of this population and concomitant differentiation to give rise to *de novo* cardiomyocytes. Cell transplantation confirmed a progenitor source and chromosome painting of labelled donor cells revealed transdifferentiation to a myocyte fate in the absence of cell fusion. Derived cardiomyocytes are shown here to structurally and functionally integrate with resident muscle; as such, stimulation of this adult progenitor pool represents a significant step towards residentcell-based therapy in human ischaemic heart disease.

Two previous studies have indicated a significant contribution of embryonic epicardial progenitor cells (EPDCs) to the cardiomyocyte lineage[3,4]. We investigated a basis for translating this myocardial potential in the adult heart. A significant problem in this regard is the lack of current adult epicardium-specific markers and authentic adult EPDC–Cre-expressing mouse strains for canonical lineage tracing. Previously reported genetic models to trace, or target, cells originating in the epicardium, such as $Wt1^{GFPCre/+}$ and $Wt1^{CreERT2/+}$; $R26R^{EYFP/+}$ mice or $Tbx18^{Cre}$ mice[3,4], cannot be applied directly to their adult counterparts, as the epicardial markers are either restricted to embryonic stages (Supplementary Fig. 1) or additionally expressed in the myocardium, as in the case of the *Tbx18* model[5]. Therefore, we sought to reactivate *Wt1* expression in the adult heart by pre-treatment ('priming') with thymosin β4 (Tβ4), which we previously showed induces adult EPDCs to form vascular precursors for neovascularization[2,6], followed by myocardial infarction (see schematic, Fig. 1a). Thus, we were able to establish both constitutive (GFP^+) and pulse (YFP^+) labelling of $Wt1^+$ progenitors to characterize the potential spatiotemporal distribution of primed adult cardiomyocyte precursors.

We initially established epicardial explants from Tβ4-primed $Wt1^{GFPCre/+}$ adult hearts (7 days of intraperitoneal injections without myocardial infarction; Supplementary Fig. 2a–d) as previously described[2,7] and investigated Isl1 expression as a marker of postnatal cardioblasts[8] along with Nkx2-5, an early marker of cardiomyocyte progenitors[9–11]. $Isl1^+$/GFP^+ cells and $Nkx2\text{-}5^+/GFP^+$ cells were prevalent within the explant cultures with mean percentage incidences of 76.7 ± 6.3% and 7.2 ± 2.1%, respectively (mean percentage ± standard error of mean (s.e.m.); $n = 12$ explants), as were progenitor-like GFP^+ cells, which expressed more mature markers of cardiomyocyte differentiation such as cardiac troponin T (cTnT, also known as Tnnt2; 4.1 ± 1.6%; Supplementary Fig. 2i, j) sarcomeric α-actinin (SαA; 4.8 ± 2.4%; Supplementary Fig. 2l, m) and cardiac myosin binding protein C (MyBPC, also known as Mybpc2; 4.6 ± 0.8, mean percentage ± s.e.m.; Supplementary Fig. 2o, p). By day 14 in culture, cells adopted a more differentiated cardiac muscle phenotype; with evidence of sarcomeric structure in conjunction with compartmentalization of the GFP signal (Supplementary Fig. 2k–r).

Next we determined the extent of *Wt1* re-expression *in vivo* alongside the quantity and distribution of GFP^+ and YFP^+ adult progenitors. With injury alone (no Tβ4 priming), expression of *Wt1* and *Tbx18* was significantly increased at day 7 after myocardial infarction, dependent on the severity of the injury (Supplementary Fig. 3a). Following Tβ4 priming, expression of both epicardial genes was precociously increased by day 2 after myocardial infarction (Supplementary Fig. 3b), and this persisted in Tβ4-primed GFP^+ cells isolated by fluorescence-activated cell sorting (FACS) at day 4 after injury (Supplementary Fig. 4a). *In situ* hybridization, at an equivalent stage, revealed an upregulation in *Wt1* expression in small round 'progenitor-like' cells within the epicardium, subepicardial region and underlying myocardium (Supplementary Fig. 4b–d).

Tβ4 priming resulted in significantly more sorted GFP^+ and YFP^+ cells from whole hearts taken at day 7 after myocardial infarction when compared to treatment with vehicle (Fig.

1b–e and Supplementary Fig. 5a–d; GFP, 6.12%+Tβ4 versus 3.38%+PBS; YFP, 0.74% +Tβ4 versus 0.36%+PBS). This was confirmed *in situ* by anti-GFP immunostaining on serial heart sections at the equivalent stage after injury (Supplementary Fig. 5e). Further flow cytometry characterization of a progenitor phenotype revealed that labelled cells, at day 4, were not c-Kit$^+$ (Supplementary Fig. 6a–e). Instead, approximately 80% were positive for stem cell antigen factor 1 (Sca-1$^+$; Supplementary Fig. 6f–j), consistent with the notion that the adult epicardium is a heterogeneous lineage[12].

Two-photon molecular excitation laser scanning microscopy revealed pulse-labelled YFP$^+$ cells in the epicardium and subepicardial region at day 7 after myocardial infarction (Fig. 1f, g), distributed in diminishing numbers towards the underlying myocardium (Fig. 1h). Proliferative Ki67$^+$ progenitors were observed in epicardial and subepicardial regions (Supplementary Fig. 7a, b) alongside YFP$^+$ cells positive for phospho-histone H3 (Supplementary Fig. 7c–f), which expanded in number from day 2–14 (Supplementary Fig. 7g–m). A subpopulation, residing in the epicardium, was positive for Isl1 and Nkx2-5 at day 2 after myocardial infarction (Fig. 1i–m and Supplementary Fig. 8a–d) and these cardiac progenitors significantly increased by day 7 after myocardial infarction (Fig. 1n). By day 14, YFP^1 cells were located within the border zone and peri-infarct region (Fig. 2a–c), which co-expressed SαA (Fig. 2d, e, h–k) and cTnT (Fig. 2f, g, l) and by virtue of their size, gross morphology and inherent ultrastructure resembled mature cardiomyocytes (Fig. 2d–l). Whereas a relatively small number of Isl1$^+$ progenitors were evident in Tβ4-primed, sham-operated hearts (Fig. 1n), we failed to locate any mature GFP$^+$/YFP$^+$ cardiomyocytes in the absence of injury (sham) or Tβ4 priming (data not shown). The *de novo* cardiomyocytes appeared appropriately integrated with the resident myocardium and with each other, as determined by both N-cadherin (Ncad)$^+$ adherens junctions (Fig. 2f–i) and connexin 43 (Cx43)$^+$ gap junction formation (Fig. 2j, k). Structurally coupled mature cTnT$^+$/YFP$^+$ cardiomyocytes were evident proximal to the scar and within the border zone (Fig. 2l). Consistent with tracking labelled cardiomyocytes from progenitors, proliferating BrdU$^+$ cells at day 4 (Supplementary Fig. 9a–d) were traced to BrdU$^+$/YFP$^+$ cardiomyocytes at day 14 (Supplementary Fig. 9e–h). The total mean percentage of YFP$^+$ progenitors that became cardiomyocytes was 0.59 ± 0.18% (serial sections through $n = 7$ hearts ±s.e.m.). The mean ratio of YFP$^+$ *de novo* cardiomyocytes to YFP$^-$ pre-existing cardiomyoctes residing in the peri-infarct region (Fig. 2b) was 0.066 (1:15; ±0.0015; six hearts analysed). In addition, from the two-photon imaging we were able to identify numbers of YFP$^+$ cardiomyocytes (192.5±12.1; four hearts analysed) in the underlying myocardium of the left ventricular wall up to a depth of ≤100 μm. Approximately 82% of YFP$^+$ cardiomyoctes were located proximal to the site of injury, residing within either the border zone or the immediate surrounding healthy myocardium (Fig. 2c, l and Supplementary Fig. 10a–c).

To assess functional integration with resident myocardium, we recorded cellular calcium transients $[Ca^{2+}]_i$ between YFP$^+$ and YFP$^-$ cells *in situ*, as previously described[13] (Fig. 2m–s and Supplementary Fig. 10a–f). Two-photon imaging confirmed migration of YFP$^+$ cells from the outer epicardial layer into the underlying myocardium (Supplementary Fig. 7m). At day 14 after myocardial infarction, evoked $[Ca^{2+}]_i$ transients in YFP$^+$ cardiomyocytes were synchronous, with kinetics indistinguishable from those of neighbouring YFP$^-$ cardiomyocytes (Fig. 2q–s). Apparent differences in resolution between resident YFP$^-$ and *de novo* YFP$^+$ cardiomyocyte transients (compare Fig. 2q with r) were observed, reflecting the newly acquired function of the YFP$^+$ population.

To rule out the possibility that we traced resident cardiomyocytes that were labelled by virtue of ectopic activation of the fluorophore from the *Wt1* knock-in alleles, we carried out a series of experiments transplanting FACS-isolated donor GFP$^+$ cells into non-transgenic host hearts. Extensive analyses indicated that the prospective donor cells were progenitors of

epicardial origin (Fig. 3). $Wt1^+$ cells were restricted to the epicardium and subepicardial region throughout the heart, as confirmed by co-staining with an antibody against podoplanin, a transmembrane glycoprotein[14] that specifically marked the epicardial and myocardial boundaries (Fig. 3a, b). Immunostaining for anti-GFP revealed GFP^+ cells residing in the expanded epicardium but excluded from the myocardium throughout the heart (Fig. 3c, e). Real-time quantitative polymerase chain reaction analyses on FACS-isolated donor cells at day 4 revealed no expression of the canonical cardiomyocyte markers cTnT, MyBPC and Actn2 (Fig. 3d). We also analysed hearts isolated from Tβ4-primed/injured $MLC2v^{Cre/+}$;$R26R^{EYFP/+}$ mice (MLC2v–YFP; Fig. 3f), which lineage-traced ventricular cardiomyocytes as YFP^+ from early developmental stages[15] to adulthood, and confirmed an absence of Wt1 in both healthy and scarred myocardium respectively (Fig. 3g, h).

In a previous study, Wt1 was shown to be expressed in the coronary vasculature after myocardial infarction in the rat heart[16]. Co-immunostaining for Wt1 or GFP with Pecam and Flk1, respectively, excluded Wt1 expression in both coronary veins and arteries within the donor hearts and ruled out the possibility of the GFP^+ progenitor population arising from existing vasculature (Fig. 3i, j). The FACS-isolated cells at day 4 revealed no expression of the canonical vascular markers Pecam and Tie2 (Fig. 3k), and cytospin with comparative immunostaining of the sorted GFP^+ and GFP^- populations (Fig. 3l) revealed that the GFP^+ cells were negative for both vascular markers Pecam and SMA and myocardial markers SαA and cTnT (Fig. 3m), whereas the GFP^- population contained cardiovascular cells (Fig. 3n).

After donor cell transplantation (Fig. 4a), GFP^+ cells within the epicardial region of the host were restricted to the site of injection after 24 h (Fig. 4b). By day 7, $GFP^+/Nkx2\text{-}5^+$ donor cells, indicative of myocardial progenitor commitment, were located proximal to the subepicardium (Fig. 4c), in conjunction with morphologically immature, $cTnT^+$ cardiomyocyte-like cells (Fig. 4d). Collectively, the presence of these staged donor derivatives suggested progressive differentiation towards a mature cardiomyocyte fate. More definitive donor GFP^+ cardiomyocytes with myofibrillar structure and that co-expressed cTnT were observed residing within the host myocardium at day 14 (Fig. 4e, f). We subsequently traced donor GFP^+ cardiomyocytes for fluorescent *in situ* hybridization (FISH) with X- and Y-chromosome paints to assess karyotype (Fig. 4a). Single XY GFP^+ cardiomyocytes were detected within the XX host, indicating that transdifferentiation had occurred in the absence of cell fusion (predicted XYXX fusion karyotype; Fig. 4g–j). To exclude the possibility of reductive divisions of fusion hybrids accounting for the XY diploid karyotype, reciprocal transplantation experiments injecting female XX GFP^+ donor cells into male XY wild-type hosts (Fig. 4k) resulted in XX $GFP^+/SαA^+$ cardiomyocytes (Fig. 4l, m) in XY host myocardium (Fig. 4n, o). Quantitative assessment of FISH on GFP^+ cardiomyocytes (total n=22) excluded the presence of a host Y chromosome in each case. Finally, we reanalysed non-transplanted YFP^+ cells in female hearts (see Fig. 2) and detected examples of both $YFP^+/cTnT^+$ (Fig. 4p) and $YFP^+/SαA^+$ (Fig. 4r) cardiomyocytes with a single XX karyotype (Fig. 4q, s).

To investigate the outcome of Tβ4 priming on cardiac function and myocardial regeneration, we carried out serial magnetic resonance imaging (MRI) 7, 14 and 28 days after myocardial infarction (Supplementary Fig. 11a–e and Supplementary Table 1). Significant improvement in functional parameters, including ejection fraction and end diastolic/systolic volumes, alongside beneficial changes in infarct/scar volume with increased left ventricular mass over time (Supplementary Table 1) were recorded with Tβ4 treatment, as a surrogate indicator of replenished myocardium (Supplementary Fig. 11f, g).

Collectively, these data indicate that the adult heart can respond to injury with a modest increase in $Wt1^+$ progenitors but without initiating a cardiogenic program. Tβ4 enhances this response, via a precocious and significant reactivation of *Wt1* expression ultimately resulting in cardiomyocyte restitution. Although we cannot unequivocally exclude the possibility that $Wt1^+$ progenitors arise from a nonepicardial source, support for an adult EPDC myocardial contribution comes from the tight regulation of $Wt1^+$ labelling in the epicardium and subepicardial region, and transplantation of donor GFP^+ progenitors residing both within and immediately proximal to the epicardium.

Reactivation of *Wt1* by injury and Tβ4 represents a robust means to faithfully tag the progression of adult cardiac progenitors to differentiated myocytes, and provides mechanistic insight into a molecular function of Tβ4 and downstream cellular events. Previously, Tβ4 was shown to upregulate ILK and Akt activity in the heart, enhancing early myocyte survival after ischaemic injury[17]. In addition, Tβ4 can induce the adult epicardium, in the same setting, to contribute coronary endothelial and smooth muscle cells and initiate vascular repair[6,18]. We now propose a further contribution, underpinning the initiation and migration of resident cardiovascular progenitors towards a cardiomyocyte fate. Although in the current study it is not possible to discriminate the relative contribution of each these proposed functions, several effects of Tβ4 seem to be delineated with time post-myocardial infarction. The pro-survival activity of Tβ4 is an early injury response to maintain the status quo of surviving myocardium, whereas the neovascularization and *de novo* cardiogenesis are longer-term regenerative functions potentially acting through the common target of adult EPDCs.

The identification of a bona fide source of myocardial progenitors is a significant step towards resident-cell-based therapy for acute myocardial infarction in human patients. The induced differentiation of the progenitor pool described into cardiomyocytes by Tβ4 is at present an inefficient process relative to the activated progenitor population as a whole. Consequently, the search is on via chemical and genetic screens to identify efficacious small molecules and other trophic factors to underpin optimal progenitor activation and replacement of destroyed myocardium.

METHODS

Generation of epicardial trace mice

$Wt1^{GFPCre/+}$ mice have been previously described[4]. Inducible $Wt1^{CreERT2/+}$;$R26R^{EYFP/+}$ mice were generated by crossing the $Wt1^{CreERT2/+}$ strain with $Rosa26R^{EYFP/+}$ reporter mice and genotyping as previously described. Adult mice were primed with intraperitoneal (i.p.) injection of Tβ4 or vehicle (PBS) into either $Wt1^{GFPCre/+}$ or $Wt1^{CreERT2/+}$;$R26R^{EYFP/+}$ (plus tamoxifen) strains. Primed mice were subsequently given a myocardial infarction by coronary artery ligation (n=85, $Wt1^{GFPCre/+}$ and n=31, $Wt1^{CreERT2/+}$;$R26R^{EYFP/+}$). Half of each myocardial infarction group were pretreated with Tβ4 and half were vehicle treated (n=6 sham-operated controls were included per experiment). Hearts were subsequently assessed using a combination of FACS, cytospin, immunofluorescence and real-time qRT–PCR analyses for GFP/YFP expression and myocardial markers after 2, 4, 7 and 14 days (see schematic in Fig. 1a). With respect to monitoring progenitor-derived cardiomyocytes the focus was on the inducible $Wt1^{CreERT2/+}$;$R26R^{EYFP/+}$ model to ensure specific temporal labelling of YFP^+ derivatives and rule out ectopic activation of the *Wt1* gene at the targeted allele. Mice that were PBS treated with tamoxifen and Tβ4 primed in the absence of tamoxifen were used as controls and importantly we never observed YFP^+ cardiomyocyte-like cells in these hearts.

Generation of MLC2v$^{Cre/+}$; R26R$^{EYFP/+}$ mice

MLC2v$^{Cre/+}$ mice have been described previously[15] and were crossed with the R26R$^{EYFP/+}$ strain to generate MLC2v–YFP mice for myocardial infarction and to exclude Wt1 upregulation in YFP^{+} cardiomyocytes.

Adult epicardial explant cultures

Adult EPDCs were prepared, as previously described[7], from 8–10-week-old Wt1$^{GFPCre/+}$ mice that had received daily i.p. injections of Tβ4 (RegeneRX, 12 mg kg^{-1} in PBS) or vehicle (PBS) for 7 days. Cells were allowed to differentiate for up to 14 days in Iscove's modified Dulbecco's medium (IMDM) containing 20% FBS, before fixing in 4% para-formaldehyde for immunostaining analysis. At the outset GFP^{+} cells were recorded emerging from Tβ4-treated explants (66.8±4.5; mean percentage of GFP^{+} cells relative to total number of cells in outgrowth ± s.e.m.; n=12 explants). Outgrowing cells, up to 6 days in culture, were documented as immature and phenotypically similar to Nkx2-5^{+} progenitors previously isolated from embryonic hearts[10] (Supplementary Fig. 2a–d). Throughout the *ex vivo* studies, PBS (vehicle)-treated explants were used as controls and revealed limited outgrowth or emergence of a significantly reduced number of GFP^{+} progenitor-like cells. The percentage incidence of GFP^{+} progenitors in the PBS treated/control explant cultures was recorded as 14.3±1.9% (mean ± s.e.m.; n=12), significantly lower ($P \leq 0.001$) than those primed by Tβ4. Importantly, vehicle-treated cells failed to adopt a myocardial fate and only isolated fibroblast-derivatives were observed in control cultures (not shown).

Despite evidence of sarcomeric marker expression (cTnT, SαA and MyBPC) after Tβ4 treatment we did not observe beating in culture of the more differentiated cardiomyocyte-like cells documented. Because spontaneous contraction *in vitro* is confined to immature fetal or neonatal cardiomyocytes[20], this may reflect a more mature adult myocyte phenotype.

Tβ4 administration

The injection regimen of Tβ4 for priming Wt1$^{GFPCre/+}$ and Wt1$^{CreERT2/+}$;R26R$^{EYFP/+}$ mice, including induction with tamoxifen is outlined in Fig. 1a. In separate experiments, MLC2v$^{Cre/+}$;R26R$^{EYFP/+}$ and wild-type C57BL/6J mice were subject to the same injection regimen for epicardial priming. Adult mice received i.p. injection of Tβ4 (12 mg kg^{-1}) or vehicle (PBS) daily for 7 days. On the eighth day Wt1$^{CreERT2/+}$;R26R$^{EYFP/+}$ mice were injected with tamoxifen (2 mg suspended in peanut oil; i.p.) to induce CreERT2/Cre expression. Further injections of Tβ4/vehicle were given on day 9 and tamoxifen on day 10. Myocardial infarction was performed 3 days after this regimen.

Myocardial infarction

Mice were housed and maintained in a controlled environment. All surgical and pharmacological procedures were performed in accordance with the Animals (Scientific Procedures) Act 1986, (Home Office, UK). For all experiments adult male Wt1$^{GFPCre/+}$ (n=85), Wt1$^{CreERT2/+}$;R26R$^{EYFP/+}$ (n=31), MLC2v$^{Cre/+}$R26R$^{EYFP/-}$ mice (n=5) and wild-type C57BL/6J mice (n=21), (25–30 g) were primed with Tβ4 or vehicle, as described earlier, before surgical procedures. Myocardial infarction was induced in isoflurane-anaesthetized mice by permanent ligation of the left anterior descending artery (LAD). Sham controls (suture passed under the LAD but not ligated) were performed in Wt1$^{GFPCre/+}$ mice (n=6) and Wt1$^{CreERT2/+}$;R26R$^{EYFP/+}$ mice (n=6). On recovery, animals received i.p. injection of Tβ4 (12 mg kg^{-1}) or vehicle (PBS). Further injections were given every second day. For pulse chase BrdU experiments, Wt1$^{GFPCre/+}$ and Wt1$^{CreERT2/+}$;R26R$^{EYFP/+}$ mice were injected i.p. with 200 μl of BrdU labelling reagent (Zymed, Invitrogen) on recovery

and at 2 and 4 days after LAD ligation. Hearts were harvested at 2, 4, 7 and 14 days after ligation and bisected transversely midway through the scar: the apex was snap frozen for RNA isolation and subsequent real-time qRT–PCR studies while the remaining tissue was fixed in 4% PFA for cryosectioning and immunostaining analyses.

GFP$^+$/YFP$^+$ cell isolation and characterization

Hearts from Wt1$^{GFPCre/+}$ and Wt1$^{CreERT2/+}$;R26R$^{EYFP/+}$ mice treated with Tβ4 or vehicle were harvested 7 days after ligation and processed by enzymatic digestion using a 0.1% collagenase II-PBS solution (Worthington Biochemicals) to achieve a single-cell suspension. GFP$^+$ or EYFP$^+$ cells were isolated from the total cardiac cell population using a Beckman Coulter MoFlo XDP cell sorter with a 488 nm laser beam to excite YFP/GFP (collected in the 530/40 nm channel) and a 355 nm laser beam used to excite DAPI (collected in the 450/50 nm channel).

To characterize GFP$^+$ cells, hearts from Wt1$^{GFPCre/+}$ mice treated with Tβ4 were harvested 4 days after ligation and processed, as described earlier, to obtain a single-cell suspension. As a control, hearts from uninjured Wt1$^{GFPCre/+}$ mice treated either with Tβ4 or with vehicle were also analysed after 7 days. Cells were incubated with the following primary and secondary antibodies: c-Kit (goat IgG, R&D System), Sca-1 (rat IgG2a, BD Pharmigen), Alexa Fluor 647 anti-goat or Alexa Fluor 647 anti-rat (Invitrogen) and analysed using a Beckman Coulter CyAn ADP analyser equipped with a 488 nm laser and 633 nm red diode and run by Summit Software. Data were analysed using the FlowJo Software.

Cell cytospins were collected using a Shandon Cytospin 3 centrifuge. Cytospun cells were then processed for immunostaining for epicardial and cardiovascular markers as described earlier.

YFP$^+$ cardiomyocytes were assessed by cell counts through serial sections. The mean percentage of YFP$^+$ progenitors that became cardiomyocytes was estimated across n=7 hearts ± s.e.m. The incidence of YFP$^+$ *de novo* cardiomyocytes relative to pre-existing myocardium was expressed as the mean ratio of YFP$^+$ cells divided by YFP$^-$ cells across serial sections per heart ± s.e.m. (n=6 hearts analysed). Cell counts were also assessed after two-photon imaging in Langendorff-perfused hearts and expressed as the mean number of YFP$^+$ cardiomyocytes per heart ± s.e.m. (n=4 hearts analysed).

Immunodetection methods

Immunofluorescence was performed on adult epicardial explant cultures, on cytospun FACS-sorted cells and on cryosections of post-myocardial infarction hearts using standard protocols with the following antibodies: GFP (Clontech and Abcam, which also detect EYFP), SαA (Sigma), cardiac MyBPC (a gift from E. Ehler and M. Gautel), cTnT, cTNI, BrdU, Isl1 and Wt1 (all Abcam), Nkx2-5 (Santa Cruz), phospho-histone H3 (Upstate), podoplanin (Fitzgerald Industries) and Ki67 (Dako). To rule out the possibility of autofluorescence accounting for the detection of either GFP or YFP protein expression, sections through the left ventricle were stained with a polyclonal anti-GFP antibody (which detects both fluorescent proteins). The specificity of the anti-GFP antibody was ascertained by immunofluorescence on non-primed, intact hearts, which detected neither labelled cells in the epicardial region, nor their derivatives (no signal; not shown).

To detect BrdU-positive nuclei, sections were treated with 2 N HCl for 30 min at room temperature (22 °C) to denature the DNA, and neutralized in 0.1 M sodium borate pH 8.5 for 12 min before incubation with the anti-BrdU antibody. Owing to the destruction of cellular antigens resulting from acid treatment, these steps were performed after the incubation with antibodies to GFP and SαA. Images were acquired using either a Zeiss

AxioImager with ApoTome or a Zeiss LSM 710 confocal microscope equipped with argon and helium neon lasers using ×20, ×40 and ×63/1.4 (oil immersion) objectives.

RNA *in situ* hybridization

RNA *in situ* hybridization on adult heart cryosections was performed as previously described[21], using a digoxigenin-labelled antisense riboprobe specific for *Wt1* (ref. 4), alongside a sense control.

RNA isolation and gene expression profiling

Total RNA was isolated from the apex of collected hearts using the Trizol reagent (Invitrogen), according to the manufacturer's instructions and reverse-transcribed using Superscript III RT (Invitrogen). Real-time qRT–PCR analysis was performed on an ABI 7900 Sequence Detector (Applied Biosystems) using SYBR Green (QuantitectTM SYBR Green PCR Kit, Qiagen). Data were normalized to Hprt expression (endogenous control). Fold-changes in gene expression were determined by the $2^{-\Delta\Delta CT}$ method[22] and are presented relative to levels in non-myocardial infarction (sham) hearts. Complementary DNA PCR primer sequences were obtained from Primer Bank (http://pga.mgh.harvard.edu/primerbank/) and details are available on request.

To characterize GFP^+ progenitors, total RNA was obtained from FACS-sorted GFP^+ cells isolated after enzymatic digestion of the hearts of the Tβ4-treated $Wt1^{GFPCre/+}$ mice at 4 and 14 days following LAD ligation using a Beckman Coulter MoFlo XDP cell sorter. Total RNA was isolated using the RNeasy Micro Kit (Qiagen), according to the manufacturer's instructions, and processed as above.

Multiphoton imaging

Multiphoton imaging was performed in Langendorff-perfused hearts loaded with Rhod- 2/AM (Invitrogen) as described previously[19] except that 50 μM blebbistatin was used to inhibit myosin crossbridge cycling and prevent movement. Spontaneous calcium transients were visualized without electrical pacing. Images were recorded using a C-apochromat×40/1.2 NA water-immersion objective on a Zeiss LSM NLO axiovert microscope coupled to a tunable Chameleon laser (Coherent) and external (nondescanned) detectors. EYFP/EGFP and Rhod-2/AM were excited simultaneously at 990 nm, which is long enough to avoid myofibril autofluorescence while strongly exciting the fluorochromes. Emitted light was collected using a bandpass 500–550 nm and 575–640 nm. Calcium transients were calculated by averaging along a line 40 pixels wide using ImageJ (http://rsbweb.nih.gov/ij) software. The ImageJ fourier filter was used to remove noise of less than 3 pixels and three-dimensional images were constructed using Imaris (Bitplane).

MRI analysis

$Wt1^{CreERT2/+}$;$R26R^{EYFP/+}$ and wild-type C57BL/6J mice treated with Tβ4 or vehicle, were subjected to MRI assessment at 7 days after LAD ligation. Where infarct size was within the range of 15–40%, follow-up MRI analysis was performed on the same mice at 14 and 28 days post-myocardial infarction, to determine temporal changes in infarct size and cardiac function. Mice were anaesthetized with isoflurane (4%), placed onto an animal cradle and maintained at 37±0.5 °C with oxygen and anaesthetics (1–2% isoflurane), supplied via a nose cone (1 l min^{-1}). Cardiorespiratory monitoring and gating were performed using an MR-compatible system (SA Instruments) with needle electrodes inserted into the front limbs and a respiratory pillow placed on the chest. Imaging was performed using a 9.4T VNMRS horizontal bore scanner (Varian) with a shielded gradient system (1,000 mT m^{-1}) using a 39 mm diameter volume coil (Rapid Biomedical GmbH). An electrocardiogram and respiratory

gated spoiled gradient echo sequence was used to acquire cine cardiac images with the following parameters for standard cine acquisitions: Time to echo (TE), 1.18 ms; time to repetition (TR), 4.5 ms; flip angle, 20°; slice thickness, 1 mm; no slice separation, field of view (FOV), 25.6 × 25.6 mm^2; matrix size, 128 × 128; number of signal averages (NSA), 2. Twenty cine-frames were recorded to cover the cardiac cycle. Infarct size was assessed using late gadolinium enhancement (LGE), as previously described[23]. Briefly, 0.6 mmol kg^{-1} Gd-DTPA was administered i.p. followed by a Look-Locker acquisition with multiple time to inversion (TI) to determine the optimum TI. This was followed by a multi-slice inversion recovery (IR) acquisition with flip angle (FA)=90° using the following imaging parameters: TE, 1.58 ms; TR, ~500–600 ms; FA, 90°; slice thickness, 0.5 mm; 0.5 mm slice gap; 7–8 slices; FOV, 25.6 × 25.6 mm^2; matrix size, 192 × 192; NSA, 2. A second stack of short-axis images offset by 0.5 mm was acquired to generate a continuous data set.

MR image analysis

Randomized and anonymized images were analysed using the cardiac analysis software Segment (http://segment.heiberg.se)[24]. To estimate the infarct size, endocardial and epicardial borders were segmented on LGE images automatically with manual adjustments followed by automatic delineation of infarct tissue using a built-in fraction of segment. Manual corrections were performed where necessary. Infarct size, expressed as percentage of left ventricular mass, was calculated as infarct volume/left ventricular volume (from cine data). Results are shown as mean±s.e.m. Comparisons between groups were performed using a repeated measures one-way ANOVA. All statistical analysis was performed using R software[25] version 2.8.1.

Cell transplantation

Adult male (n=14) and female (n=14) $Wt1^{GFPCre/+}$ mice were primed with Tβ4 and myocardial infarction was induced as described earlier. Pooled GFP^+ progenitors were isolated (from eight surviving donors) using a Beckman Coulter MoFlo XDP cell sorter after enzymatic digestion of the hearts of Tβ4-treated $WT1^{GFPCre/+}$ mice 4 days after ligation. Female (n=3) and male (n=3) non-transgenic mice were treated with Tβ4 before surgery and myocardial infarction was induced as described above. 3–6 × 10^4 FACS-sorted male GFP^+ cells, resuspended in 10 μl of DMEM, were injected into the subepicardial space of the female host hearts (n=3) immediately after LAD ligation. On recovery, animals received i.p. injection of Tβ4 (12 mg kg^{-1}). Further injections were given every second day and hearts were harvested 14 days post-myocardial infarction and processed for immunofluorescence analysis as described earlier. In the second set of experiments, 5×10^4 FACS-sorted female GFP^+ cells, resuspended in 10 μl of DMEM, were injected into the subepicardial space of the male host hearts (n=3) immediately after LAD ligation. On recovery, animals received i.p. injection of Tβ4 (12 mg kg^{-1}). Further injections were given every second day and hearts were harvested at 24 h, 7 days and 14 days post-myocardial infarction and processed for immunofluorescence analysis.

FISH

After immunofluorescence analysis of EPDC-derived cardiomyocytes in adult heart cryosections, as described earlier, images were acquired before FISH. FISH was performed using mouse StarFISH probes (Cambio), essentially according to the manufacturer's instructions, with the following modifications: muscle was digested in 0.025% pepsin for 40 min at 37 °C. After dehydration, tissue sections were denatured by immersion in 70% formamide at 72 °C for 5 min. Cy3-conjugated X- and FITC-conjugated Y-chromosome paints were mounted, sealed under coverslips and denatured by incubation at 60 °C for 10 min before hybridization in a humid chamber overnight at 37 °C. Coverslips were removed and sections were either washed, according to the manufacturer's instructions, or, where Y-

chromosome probes were used, a FITC amplification kit (Cambio) was used, according to the manufacturer's instructions.

Supplementary Material

Refer to Web version on PubMed Central for supplementary material.

Acknowledgments

This work was funded by the British Heart Foundation. We are grateful to F. Costantini and S. Srinivas for providing the R26R–EYFP mouse strain, to B. Vernay for assistance with confocal microscopy and A. Eddaoudi, P. Chana and A. Angheluta for assistance in flow cytometry. We thank A. Taylor and V. Muthurangu for functional interpretation of MRI data and RegeneRx Biopharmaceuticals for provision of clinical grade Tβ4.

References

1. Willems E, Bushway PJ, Mercola M. Natural and synthetic regulators of embryonic stem cell cardiogenesis. Pediatr. Cardiol. 2009; 30:635–642. [PubMed: 19319460]
2. Smart N, et al. Thymosin β4 induces adult epicardial progenitor mobilization and neovascularization. Nature. 2007; 445:177–182. [PubMed: 17108969]
3. Cai CL, et al. A myocardiallineage derives from *Tbx18* epicardialcells. Nature. 2008; 454:104–108. [PubMed: 18480752]
4. Zhou B, et al. Epicardial progenitors contribute to the cardiomyocyte lineage in the developing heart. Nature. 2008; 454:109–113. [PubMed: 18568026]
5. Christoffels VM, et al. Tbx18 and the fate of epicardial progenitors. Nature. 2009; 458:E8–E9. [PubMed: 19369973]
6. Bock-Marquette I, et al. Thymosin β4 mediated PKC activation is essential to initiate the embryonic coronary developmental program and epicardial progenitor cell activation in adult mice *in vivo*. J. Mol. Cell. Cardiol. 2009; 46:728–738. [PubMed: 19358334]
7. Smart N, Riley PR. Derivation of epicardium-derived progenitor cells (EPDCs) from adult epicardium. Curr. Protoc. Stem Cell Biol. 2009 Unit 2C.2.
8. Laugwitz KL, et al. Postnatal isl1^{+} cardioblasts enter fully differentiated cardiomyocyte lineages. Nature. 2005; 433:647–653. [PubMed: 15703750]
9. Moretti A, et al. Multipotent embryonic Isl1^{+} progenitor cells lead to cardiac, smooth muscle, and endothelial cell diversification. Cell. 2006; 127:1151–1165. [PubMed: 17123592]
10. Wu SM, et al. Developmental origin of a bipotential myocardial and smooth muscle cell precursor in the mammalian heart. Cell. 2006; 127:1137–1150. [PubMed: 17123591]
11. Prall OW, et al. An Nkx2-5/Bmp2/Smad1 negative feedback loop controls heart progenitor specification and proliferation. Cell. 2007; 128:947–959. [PubMed: 17350578]
12. Limana F, et al. Myocardial infarction induces embryonic reprogramming of epicardial c-kit^{+} cells: role of the pericardial fluid. J. Mol. Cell. Cardiol. 2010; 48:609–618. [PubMed: 19968998]
13. Rubart M, et al. Two-photon molecular excitation imaging of Ca^{2+} transients in Langendorff-perfused mouse hearts. Am. J. Physiol. Cell Physiol. 2003; 284:C1654–C1668. [PubMed: 12584115]
14. Mahtab EA, et al. Cardiac malformations and myocardial abnormalities in podoplanin knockout mouse embryos: correlation with abnormal epicardial development. Dev. Dyn. 2008; 237:847–857. [PubMed: 18265012]
15. Chen J, Kubalak SW, Chien KR. Ventricular muscle-restricted targeting of the RXRα gene reveals a non-cell-autonomous requirement in cardiac chamber morphogenesis. Development. 1998; 125:1943–1949. [PubMed: 9550726]
16. Wagner KD, et al. The Wilms' tumor suppressor *Wt1* is expressed in the coronary vasculature after myocardial infarction. FASEB J. 2002; 16:1117–1119. [PubMed: 12039855]
17. Bock-Marquette I, et al. Thymosin β4 activates integrin-linked kinase and promotes cardiac cell migration, survival and cardiac repair. Nature. 2004; 432:466–472. [PubMed: 15565145]

18. Smart N, et al. Thymosin β4 facilitates epicardial neovascularization of the injured adult heart. Ann. N. Y. Acad. Sci. 2010; 1194:97–104. [PubMed: 20536455]
19. Rubart M, et al. Two-photon molecular excitation imaging of Ca^{2+} transients in Langendorff-perfused mouse hearts. Am. J. Physiol. Cell Physiol. 2003; 284:C1654–C1668. [PubMed: 12584115]
20. Ieda M, et al. Direct reprogramming of fibroblasts into functional cardiomyocytes by defined factors. Cell. 2010; 142:375–386. [PubMed: 20691899]
21. Moorman AF, et al. Sensitive nonradioactive detection of mRNA in tissue sections: novel application of the whole-mount *in situ* hybridization protocol. J. Histochem. Cytochem. 2001; 49:1–8. [PubMed: 11118473]
22. Livak KJ, Schmittgen TD. Analysis of relative gene expression data using real-time quantitative PCR and the $2^{-\Delta\Delta CT}$ method. Methods. 2001; 25:402–408. [PubMed: 11846609]
23. Price A, et al. Lategadolinium enhanced MRI in small animal models of myocardial infarction. J. Cardiovasc. Magn. Reson. 2010; 12(Suppl. 1):P98.
24. Heiberg E, et al. Time resolved three-dimensional automated segmentation of the left ventricle. Comput. Cardiol. 2005; 32:599–602.
25. Ihaka R, Gentleman R. R: a language for data analysis and graphics. J. Comput. Graph. Stat. 1996; 5:299–314.

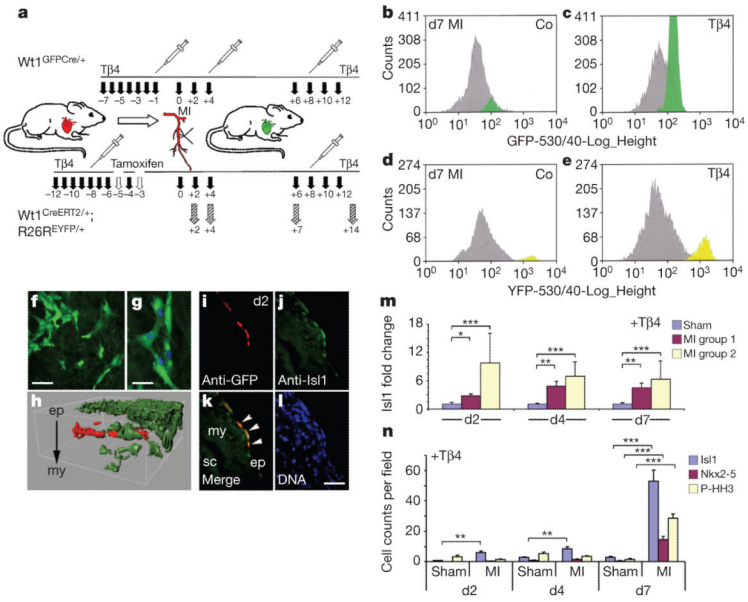

Figure 1. Activated Wt1^{+} cells give rise to cardiac progenitors in the injured adult heart

a, Schematic of constitutive or pulse-chase labelling of Wt1^{+} cells. **b–e**, FACS analyses of whole hearts at day 7 (d7) after myocardial infarction (MI) revealed a significant increase in GFP^{+} (**b, c**) and YFP^{+} (**d, e**) cells following priming with Tβ4, as compared to PBS-treated controls (Co); *x*-axes represent either GFP (**b, c**) or YFP (**d, e**) fluorescent wavelengths on a logarithmic scale and *y*-axes represent total cell numbers isolated by FACs (**b–e**). **f, g**, Multi-photon imaging at day 7 after myocardial infarction revealed YFP^{+} cells within the epicardium and subepicardial region migrating towards underlying myocardium. Scale bars in **f**, 20 μm; g, 10 μm. **h**, Three-dimensional Imaris reconstruction of migrating YFP^{+} cells (green) amidst non-labelled cells (red). ep, epicardium; my, myocardium. **i–l**, YFP^{+} cells that co-stained for Isl1 (highlighted by white arrowheads in **k**) resided in the epicardium proximal to areas of scarred myocardium 2 days (d2) after myocardial infarction. sc, scar region. Scale bar in **l** (also applies to **i–l**), 50 μm. **m**, Significant increase in *Isl1* expression in primed hearts at days 2, 4 and 7 after myocardial infarction relative to sham-operated controls $*P \leq 0.05$, $*P \leq 0.01$, $***P \leq 0.001$; MI group 1 and group 2 versus sham; myocardial infarction categories: purple, mild injury; cream, severe injury; n=6 hearts per sham and MI groups. **n**, Significant increases in Isl1^{+}/YFP^{+} cells at days 2 ($*P \leq 0.05$), 4 ($**P \leq 0.01$) and 7 ($***P \leq 0.001$) after myocardial infarction and Nkx2-5^{+}/YFP^{+} cells by day 7 ($***P \leq 0.001$) alongside phospho-histone H3^{+} (P-HH3^{+}) proliferating YFP^{+} progenitors at day 7 ($***P \leq 0.001$), compared to sham-operated controls. *P* values were calculated by Student's *t*-test (**m**) and paired ANOVA (**n**). Error bars represent mean±s.e.m. *N* values are numbers of hearts analysed for each group: N=3 (**m**); N=4 (d2 and d4) and N=7 (d7) (**n**).

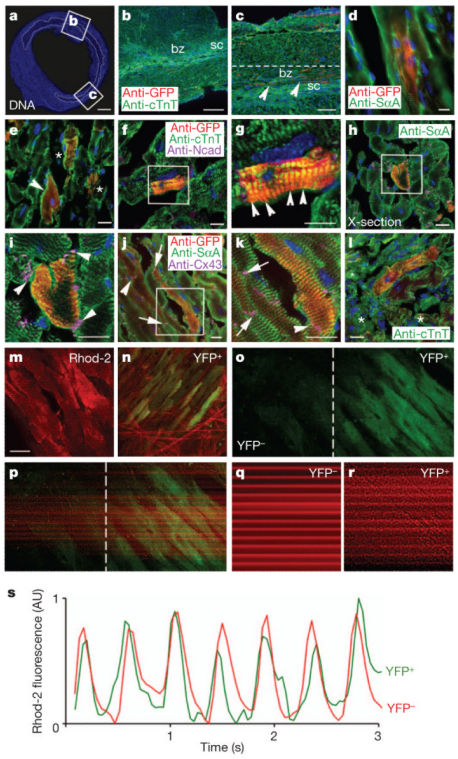

Figure 2. Activated adult Wt1^{+} progenitors differentiate into structurally coupled cardiomyocytes

a–c, At day 14, YFP^{+} cells that co-expressed cTnT resided in the left ventricular wall within the border zone (white arrowheads in **c**; dashed white line demarcates extent of peri-infarct region). bz, border zone, sc, scar region. **d, e**, YFP^{+} cells expressing SαA as determined by epifluorescence (**d**) and confocal microscopy (**e**; white arrowhead highlights mature YFP^{+} cardiomyocyte; white asterisks highlight less mature YFP^{+} cardiomyocytes). **f, g**, Mature YFP^{+} cardiomyocytes stained positive for cTnT with sarcomeric banding (white arrowheads). **f–k**, Evidence of structural coupling between YFP^{+} and resident YFP$^{−}$ cardiomyocytes through Ncad^{+} adherens junction (white arrowhead in **i**) and Cx43^{+} gap junction formation (white arrowhead/arrows in **j, k**). **l**, YFP^{+}/cTnT^{+} cardiomyocytes were located adjacent to necrotic myocardium within the scar (white asterisks). **m, n**, Rhod-2 loading of distal YFP$^{−}$ cardiomyocytes (**m**) was compared against YFP^{+} cardiomyocytes within the peri-infarct region (**n**). **o, p**, Calcium transients across clustered YFP$^{−}$ and YFP^{+} cardiomyocytes as evidence of functional coupling. **q, r**, Distal YFP$^{−}$ spontaneous calcium transients (**q**) were compared against YFP^{+} transients (**r**). **s**, Representative traces plotted per cardiac cycle (AU, arbitrary units). All scale bars are 20 μm, except for **a**, 100 μm; **b**, 150 μm; and **c**, 150 μm. Scale bar in **m** applies to **m–r**.

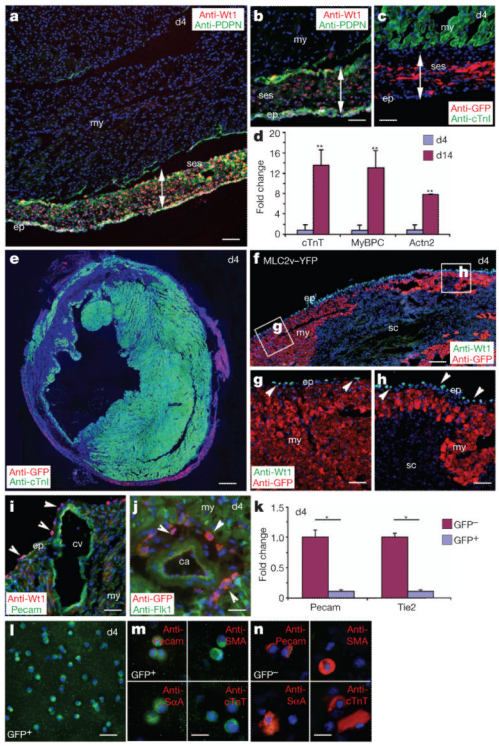

Figure 3. Prospective donor Wt1^{+}/GFP^{+} cells at day 4 after myocardial infarction seem to be derived from epicardium

a, b, Immunostaining for Wt1 and anti-podoplanin (PDPN) revealed that the day 4 donor Wt1^{+} cells were restricted to the epicardium and subepicardial space. ep, epicardium; my, myocardium; sc, scar; ses, subepicardial space. **c, e**, Anti-GFP and anti-cTnI co-staining revealed spatial restriction to the equivalent epicardial regions as for Wt1 staining with exclusion from the myocardium. **d**, cTnT, MyBPC and Actn2 were not expressed in the FACS GFP^{+} population at day 4 after myocardial infarction, whereas expression of all three myocardial markers was significantly upregulated in GFP^{+} cells at day 14 consistent with contribution of *de novo* cardiomyocytes. **f–h**, Wt1^{+} cells were restricted to the epicardium and excluded from MLC2v–YFP^{+} ventricular cardiomyocytes in regions of healthy (**g**) and scarred (**h**) myocardium. **i–k**, Expression of Wt1/GFP was excluded from within the Pecam^{+}/Flk1^{+} coronary vasculature (**i, j**; cv, coronary vein; ca, coronary artery) and confirmed by a lack of expression of Pecam and Tie2 in the day 4 GFP^{+} FACS population (**k**). **l, m**, Cytospin/immunostaining revealed a homogeneous GFP^{+} fraction at day 4, without contamination from GFP^{-} cells (**l**), which lacked vascular (Pecam and SMA) and myocardial (SαA, cTnT) markers (**m**) as compared to the GFP^{-} fraction (**n**). *$P \leq 0.05$, **$P \leq 0.01$, all statistics by Students *t*-test. Error bars represent mean ± s.e.m., *N* values are numbers of hearts analysed for each group: *N*=6 (day 4) and *N*=7 (day 14) (**d**); *N*=6 (**k**). All scale bars are 50 μm, except **a, e**, 500 μm; **f**, 200 μm; **m, n**, 20 μm.

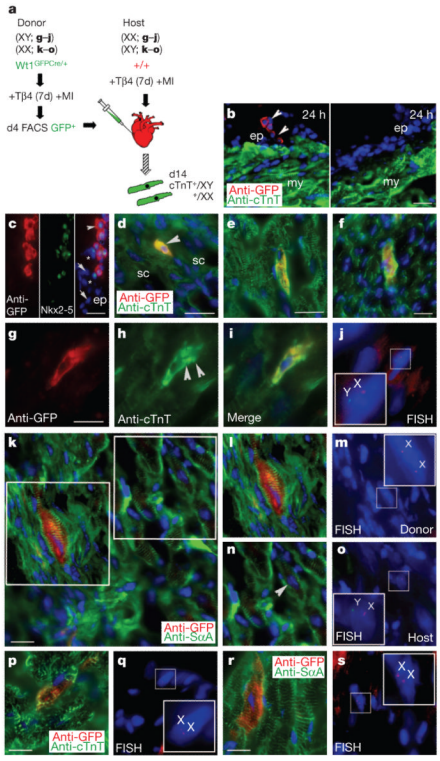

Figure 4. Transplanted donor Wt1^{+} progenitors differentiate into cardiomyocytes within host myocardium in the absence of cell fusion

a, Schematic of cell transplantation regimen. **b**, After 24 h post-transplantation GFP^{+} cells within the epicardium and subepicardial region at the injection site were absent in remote regions. ep, epicardium; my, myocardium. **c**, Transplanted GFP^{+} cells expressed Nkx2-5, indicative of a myocardial progenitor phenotype (white arrowhead highlights a GFP^{+}/Nkx2-5^{+} progenitor; white arrows highlight GFP^{-}/Nkx2-5^{+} progenitors and asterisks highlight epicardium cells negative for both GFP and Nkx2-5). **d–f**, Donor GFP^{+} cells with an intermediate differentiated phenotype (highlighted by white arrowhead, **d**), alongside those with evidence of sarcomeric banding that co-expressed cTnT were observed within host myocardium (**e, f**). sc, scar. **g–j**, GFP^{+}/cTnT^{+} cardiomyocytes (**g–i**) with sarcomeric banding (highlighted by white arrowheads in **h**) were traced for FISH analyses to reveal a single XY karyotype (**j**). X, X chromosome; Y, Y chromosome. **k–o**, Reciprocal transplantation (XX into XY) followed by confocal microscopy (**k**) revealed GFP^{+} cardiomyocytes (**l**) that had the donor XX karyotype (**m**) relative to the XY karyotype of host GFP^{-} cardiomyocytes (highlighted by white arrowhead; **n, o**). **p–s**, In female Wt1$^{CreERT2/+}$;R26R$^{EYFP/+}$ mice, previously tracked YFP^{+} cTnT^{+} (**p**) and SαA^{+} cardiomyocytes (**r** and examples shown in Fig. 3), had an XX karyotype (white box insets) supporting transdifferentiation in the absence of cell fusion with resident cardiomyocytes (**q, s**). Scale bars: **c**, 25μm; **d–f**, 20 μm; **g** (applies to **g–j**), **k** (applies to **k–o**), **p** (applies to **p–q**), **r** (applies to **r–s**), 10 μm.